ELSEVIER

Journal of Hazardous Materials 74 (2000) 25–35

Journal of Hazardous Materials

www.elsevier.nl/locate/jhazmat

Chemical speciation of nickel in fly ash by phase separation and carbon paste electrode voltammetry

Anhua Liu, John L. Wong *

Department of Chemistry, University of Louisville, Louisville, KY 40292, USA

Abstract

In a risk-based approach to cost-effective management of power plant emissions, chemical speciation of fly ash is required. A quantitative but indirect separation of nickel phases by sequential extraction was undertaken in conjunction with direct analysis of the sulfidic nickel phase by carbon paste electrode voltammetry (CPEV). Four ash samples produced in a laboratory combustion system from burning high- and low-sulfur residual oil at excess O_2 of 1 and 2–3 mol% were studied. The extractions yielded five phases of nickel. The CPEV analysis of sulfidic nickel in the ash and extraction residues was performed in pH 5 acetate. The anodic peak (-0.1 V) unique to Ni_3S_2, distinguishing it from NiS and NiS_2, was found to be absent from these ash samples. The CPEV method was consistent with phase extraction, which showed $NiSO_4$ being predominant with very low proportions of sulfidic nickel.

Keywords: Nickel speciation; Ash; Carbon paste electrode; Voltammetry; Extraction

1. Introduction

In a recent notice in the Federal Register [1], nickel and nickel compounds were to be reviewed for considering a change in the current listing of these substances to a higher alert category of ''Known to be a Human Carcinogen'' in the Ninth Report on Carcinogens. The assumption is often made that all soluble and insoluble nickel

* Corresponding author. Tel.: +1-502-852-6611; fax: +1-502-852-8149.
E-mail address: jlwong@louisville.edu (J.L. Wong).

0304-3894/00/$ - see front matter
PII: S0304-3894(99)00196-X

Table 1
Nickel speciation of EERC ash samples and SRM 1633b by five-step phase separation

Extraction step	1633b		EERC #1		EERC #2		EERC #3		EERC #4	
	Ni ug/g	% of the total Ni	Ni ug/g	% of the total Ni	Ni ug/g	% of the total Ni	Ni ug/g	% of the total Ni	Ni ug/g	% of the total Ni
1	33.2	27.6	65,601.0	74.2	26,197.4	78.7	69,632.1	92.3	33,630.2	89.8
2	46.5	38.6	20,810.9	23.5	5512.9	16.6	4615.0	6.1	2012.9	5.4
3	7.1	5.9	267.0	0.3	162.7	0.5	107.6	0.1	75.7	0.2
4	22.8	18.9	1027.7	1.2	547.4	1.6	653.1	0.9	690.4	1.8
5	10.8	9.0	673.3	0.8	854.3	2.6	443.2	0.6	1041.1	2.8
Total Ni	120.4	100.0	88,379.9	100.0	33,274.7	100.0	75,451.0	100.0	37,450.3	100.0
Ni total digestion	120.6		92,350.1		33,872.2		76,875.9		39,144.1	
Mass balance	99.8%		95.7%		98.2%		98.1%		95.6%	

compounds are carcinogenic for regulation purposes. However, in animal chronic inhalation studies of the National Toxicology Program [2], there was clear evidence for carcinogenicity for nickel subsulfide in rats but no such evidence was found for nickel sulfate in rats or mice. That various nickel compounds may pose different carcinogenic risks have provided the impetus for nickel speciation of fly ash. Our goal is to produce a new nickel species database for cost-effective management of their environmental releases. We have described phase fractionation of ash for indirect nickel speciation, allowing comparison of their nickel distribution and bioavailability [3]. For the present ash study, a five-step nickel extraction was adapted from this fractionation scheme to yield five major phases: nickel sulfate, nickel oxide–iron oxide, metallic Ni^{o}, sulfidic nickel, and nickel oxide-silica. Further subspeciation of the sulfidic nickel phase is of interest in regard to human exposure and adverse health effects; especially the presence of Ni_3S_2 is of primary concern [4]. We have reported a carbon paste electrode (CPE) voltammetric analysis of the nickel sulfide standards and reference materials [5]. The solid state CPE containing the analyte and carbon powder with paraffin oil as binder was used as the working electrode in anodic stripping voltammetry. A convergence of the

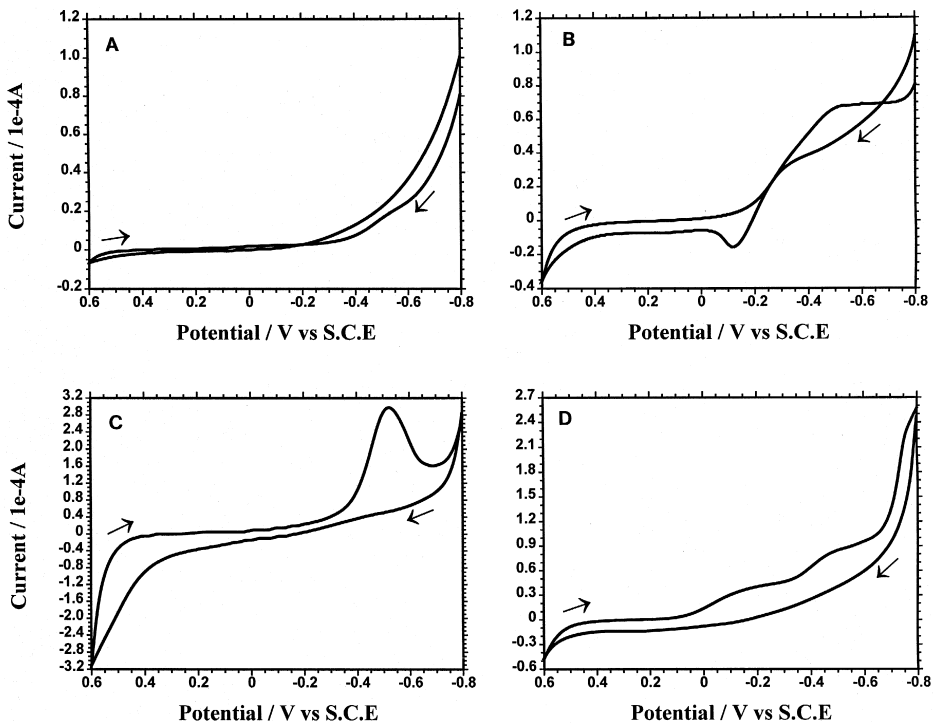

Fig. 1. CPEV of (A) $NiSO_4$, (B) Ni_3S_2, (C) NiS (millerite), and (D) NiS_2 in 1 M NaOAc–0.5 M HOAc (pH 5.0), with $E_i = -0.8$ V, $t_a = 2$ s, $v = 50$ mV/s. Blank CPE gave a flat baseline at zero current in the range of -0.5 to $+0.6$ V.

above two approaches in the nickel speciation of four residual oil ash samples was observed as presented herein.

2. Experimental

The five-step sequential extraction procedure applied to the ash samples was adapted from the nickel fractionation scheme described previously [3]. Briefly, the procedure included Step 1: 1 M NaOAc–0.5 M HOAc, pH 5, 25°C, in Bransonic bath; Step 2: 0.3 M $Na_2S_2O_4$–0.2 M citrate, pH 5, 60°C, in Bransonic bath; Step 3: electromagnet; Step 4: 30% H_2O_2–0.02 M HNO_3, pH 2, 85°C; and Step 5: 50% HF, microwave digestion. The one-step digestion for total nickel determination made use of the same conditions as in Step 5. The Ni^{2+} in the aqueous extracts was quantitated by adsorptive stripping voltammetry as Ni-dimethylglyoximate on a hanging mercury drop electrode using a CH-620 electroanalyzer in the square wave mode.

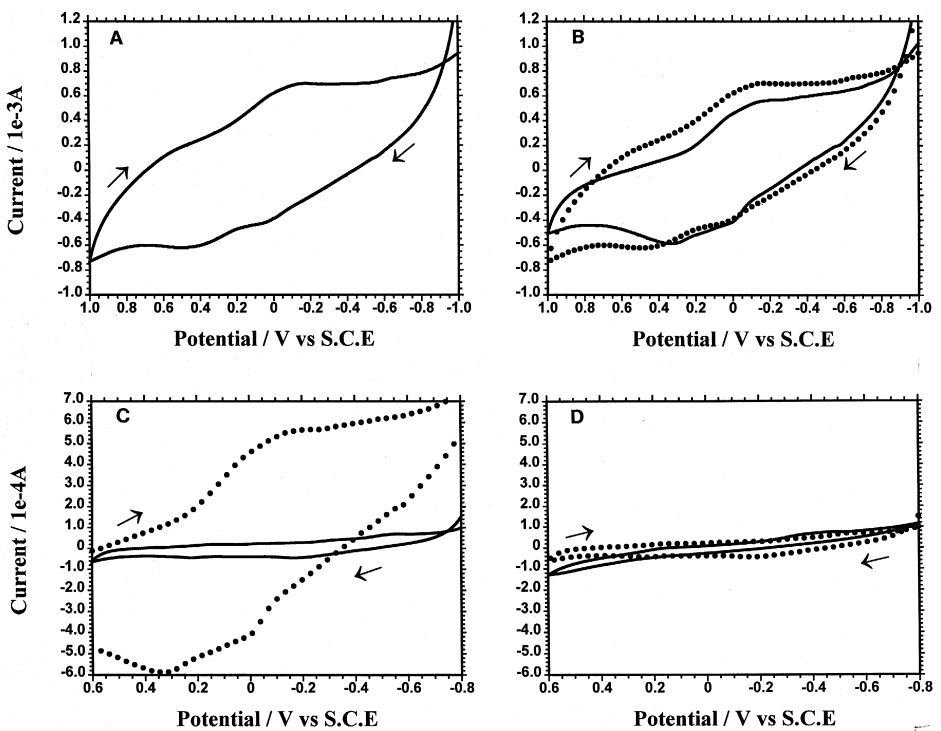

Fig. 2. CPEV of EERC #1 ash and its extraction residues: (A) EERC #1 ash, (B) Step 1 residue, (C) Step 2 residue, and (D) Step 4 residue in 1 M NaOAc–0.5 M HOAc (pH 5.0), with E_i (initial) = −1.0 V to E_t (terminal) = +1.0 V for A, B, and E_i −0.8 V to E_t +0.6 V for C, D, $t_a = 2$ s, $\upsilon = 50$ mV/s. Each residue plot in solid line is overlaid on a dotted trace of the previous plot.

Carbon paste electrode voltammetric (CPEV) analysis made use of the same electroanalyzer. The CPE body was a pipette tip (200–1000 μl size) made of virgin polypropylene with its tip cut to leave ca. 5 mm inner diameter. A 4-mm glassy carbon disc sealed in a 5-mm outer diameter Teflon tube was inserted into the tip leaving a depression in which to press in the carbon paste mixture. The paste surface was polished on writing paper. The disk-shaped CPE showed a smooth surface under a 10× microscope, and it measured about 5 mm in diameter by 0.1 mm in thickness with an area of 19.6 mm^2. A typical CPE, e.g., the Ni_3S_2-CPE, contained Ni_3S_2 (35 μg), graphite carbon (3.5 mg), and paraffin oil (2.3 μl). A blank CPE constructed in this manner gave a flat baseline with ~0 current between −0.5 and +0.6 V, and hence acceptable in accordance with the established CPE technique [6].

The chemicals were purchased from Aldrich Chemical unless otherwise noted. Four residual oil ash samples were received from the Environmental and Energy Research Center (EERC), where No. 6 residual fuel oil was burned in a laboratory-scale combustion system. The ash sampled was used in a study of the effects of sulfur in the fuel oil and air-to-fuel ratio on nickel emissions as reported by Galbreath et al. [7].

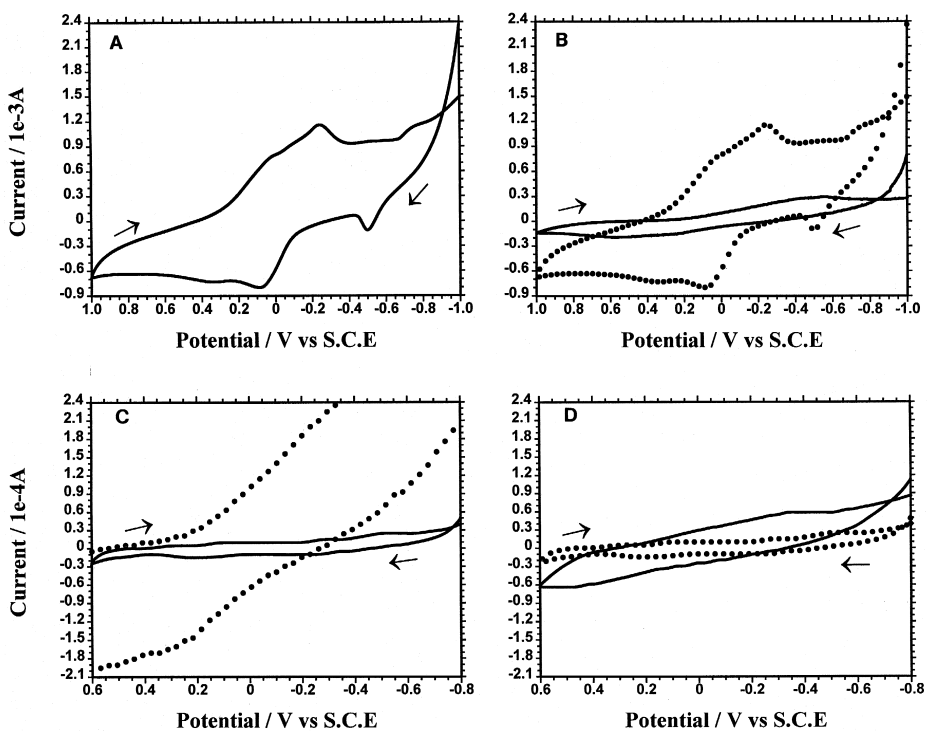

Fig. 3. CPEV of EERC #2 ash and its extraction residues: (A) EERC #2 ash, (B) Step 1 residue, (C) Step 2 residue, and (D) Step 4 residue in 1 M NaOAc–0.5 M HOAc (pH 5.0), with E_i (initial) = −1.0 V to E_t (terminal) = +1.0 V for A, B, and E_i −0.8 V to E_t +0.6 V for C, D, t_a = 2 s, υ = 50 mV/s. Each residue plot in solid line is overlaid on a dotted trace of the previous plot.

3. Results

EERC ash samples #1 and #3 were obtained from the combustion of high-sulfur (1.80 wt.%) residual oil at excess O_2 concentrations of 1 and 2 mol%, respectively. Samples #2 and #4 were obtained from the combustion of low-sulfur (0.33 wt.%) residual oil at excess O_2 concentrations of 1 and 3 mol%, respectively. The high-sulfur oil contained about twice as much Ni as the low-sulfur oil: 86 vs. 40 ppm [7]. These samples were subjected to sequential extraction-adsorptive stripping voltammetry analysis, and each sample was analyzed in duplicate along with a standard ash, SRM 1633b, for quality control. The extractions were run on duplicate ash samples, and their weights (mg) were as follows: SRM 1633b 29.4, 33.7; EERC #1 21.7, 25.0; EERC #2 39.4, 10.9; EERC #3 26.5, 26.1; and EERC #4 26.1, 23.0. The total nickel determination was carried out in a separate run to provide a check on the mass balance as part of quality assurance. The data summarized in Table 1 are the mean values of two sets of nickel speciation results.

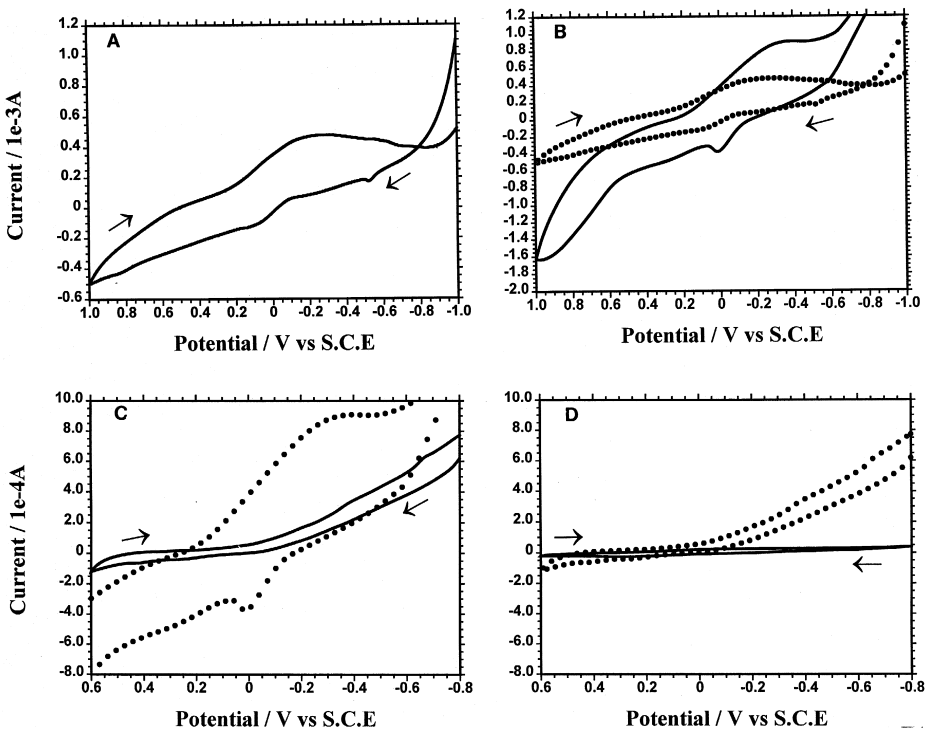

Fig. 4. CPEV of EERC #3 ash and its extraction residues: (A) EERC #3 ash, (B) Step 1 residue, (C) Step 2 residue, and (D) Step 4 residue in 1 M NaOAc–0.5 M HOAc (pH 5.0), with E_i (initial) = −1.0 V to E_t (terminal) = +1.0 V for A, B, and E_i −0.8 V to E_t +0.6 V for C, D, $t_a = 2$ s, $\upsilon = 50$ mV/s. Each residue plot in solid line is overlaid on a dotted trace of the previous plot.

The CPEV analysis was performed on nickel standards and the four EERC ash samples, including their extraction residues. These residues were generated independent of the experiments in Table 1. The CPEV results are given in Figs. 1–6. Fig. 1 shows four CPE cyclic voltammograms (CV): (A) $NiSO_4$, 4.0 mg; (B) Ni_3S_2, 3.5 mg; (C) NiS (millerite), 0.69 mg; and (D) NiS_2 (Johnson Matthey), 1.2 mg; determined in 1 M NaOAc–0.5 M HOAc (pH 5.0) in the potential range from -0.8 to $+0.6$ V, with initial scanning potential $(E_i) = -0.8$ V, accumulation time $(t_a) = 2$ s, scan rate $(\upsilon) = 50$ mV/s. All potentials are reported with respect to saturated calomel electrode. Each CPE contained 3.5 mg C and 2.7 μl oil, and the blank CPE used as control gave a flat baseline. Reproducibility was achieved with coefficients of variation for peak currents and potentials of $< 10\%$. Fig. 2 shows the CV of EERC #1 ash and its extraction residues: (A) EERC #1 ash, (B) Step 1 residue, (C) Step 2 residue, and (D) Step 4 residue, determined under similar conditions to those described for Fig. 1. These CPE contained 10 mg of the ash analyte, 10 mg C and 10 μl oil. The CV before (dotted line) and after (solid line) phase extraction are compared in the same plot to indicate change in the electroactive components due to extraction. Similarly, Figs. 3–5 show the respective CV of the other three oil ash samples and their extraction residues. Fig. 6

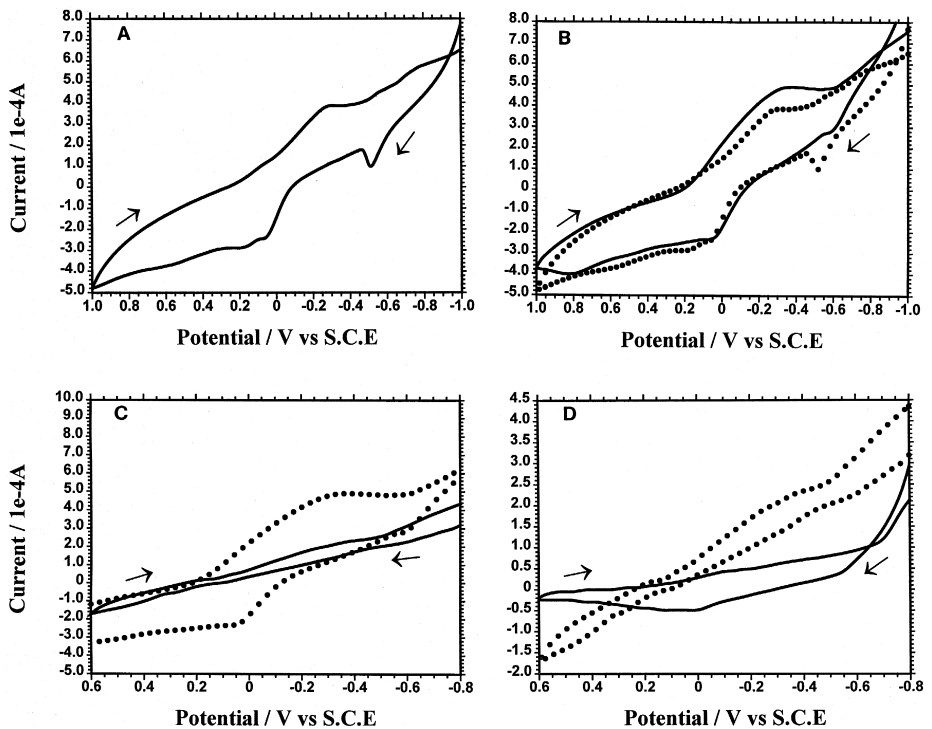

Fig. 5. CPEV of EERC #4 ash and its extraction residues: (A) EERC #4 ash, (B) Step 1 residue, (C) Step 2 residue, and (D) Step 4 residue in 1 M NaOAc–0.5 M HOAc (pH 5.0), with E_i (initial) $= -1.0$ V to E_t (terminal) $= +1.0$ V for A, B, and E_i -0.8 V to E_t $+0.6$ V for C, D, $t_a = 2$ s, $\upsilon = 50$ mV/s. Each residue plot in solid line is overlaid on a dotted trace of the previous plot.

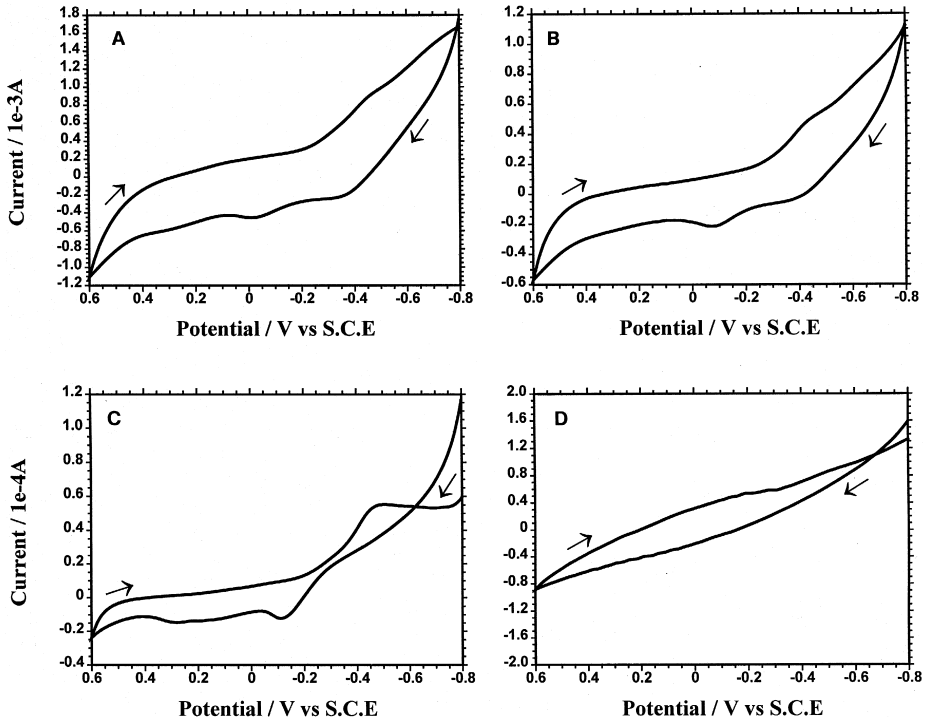

Fig. 6. CPEV of the extraction residues of EERC #1 ash spiked with 10% Ni_3S_2: (A) Step 1 residue of spiked mixture, (B) Step 2 residue, (C) Step 3 residue, and (D) Step 4 residue, in 1 M NaOAc–0.5 M HOAc (pH 5.0), with $E_i = -0.8$ V, $t_a = 2$ s, $v = 50$ mV/s.

shows the CV of the extraction residues of a mixture of 10 mg of EERC #1 ash with 1 mg Ni_3S_2: (A) Step 1 residue of spiked mixture, (B) Step 2 residue, (C) Step 3 residue, and (D) Step 4 residue, determined under the same conditions as described in Fig. 1. The CPE was made up of the spiked analyte in 10 mg C and 10 μl oil.

4. Discussion

The nickel phase fractionation scheme for oil fly ash has undergone extensive quality assurance testing as described previously [3]. In Step 1, sodium acetate solution at pH 5 removes soluble nickel compounds such as $NiSO_4$. In Step 2, sodium citrate-dithionite solution at pH 5 extracts nickel in the iron oxide matrix. Step 3 removes metallic nickel by an electromagnet. In Step 4, sulfidic nickel is released by the acidic hydrogen peroxide solution. The last Step 5 makes use of HF to release the recalcitrant nickel oxide, which may be remaining in the silica matrix.

The ash produced by EERC was derived from No. 6 fuel oil, a residual oil used by ~ 90% of oil-fired power plants [8]. Table 1 shows the five nickel phases, total nickel from a separate one-step digestion, the mass balance for the four EERC ash samples and

SRM 1633b, a standard coal ash. The mean values given in the table are from duplicate analysis with agreement within 18%, indicating sample inhomogeneity as noted before [3]. The nickel recoveries from the five separate extractions range from 95.6% to 99.8% of the total nickel, showing satisfactory precision in nickel speciation. With regard to subsequent analysis by CPEV, the following points are noteworthy. (1) The high-sulfur oil ashes, #1 and #3, contained twice as much total nickel as the low-sulfur oil ashes, #2 and #4, consistent with the nickel content ratio of the two residual oils. (2) The soluble nickel sulfate phase, 74.2–92.3% of the total Ni from Step 1, was the dominant species among the four oil ashes, unlike the standard coal ash 1633b. The same EERC samples were examined by X-ray absorption fine structure (XAFS) spectroscopy, identifying $NiSO_4$ as predominant [7]. (3) The sulfidic nickel was a minor species in the four oil ashes, accounting for $< 2\%$ of the total Ni. When high sulfur in the fuel oil was combined with higher excess O_2 (2 mol%) in producing #3 ash, sulfate was present at its highest level (92.3% of the total Ni), with formation of nickel sulfides depressed (0.9% of the total Ni).

The CPEV analysis of the ash samples is based on the characteristic anodic peak of Ni_3S_2 [5]. The CV of the standards $NiSO_4$, Ni_3S_2, NiS, and NiS_2, which were highly reproducible, are shown in Fig. 1. The cathodic peak at -0.5 V, possibly from reduction of the oxidized species generated during the anodic scan to $+0.6$ V, was given by NiS and Ni_3S_2. However, the anodic peak at about -0.1 V was unique to Ni_3S_2 [5]. Thus, analysis of the CV of the ash and extraction residues in Figs. 2–5 is focused on this anodic peak. Since Step 3 for electromagnetic removal of metallic nickel yielded relatively small amounts of Ni from these oil ash samples as shown in Table 1, this step was omitted in the CPEV analysis due to limitation of sample amounts. To show the change in voltammetric behavior after extraction, each residue plot is shown in solid line with an overlay of the previous CV plot in a dotted trace. The plots of EERC ash #1 (from oil with sulfur 1.8 wt.% at excess O_2 1 mol%) and ash #2 (from oil with sulfur 0.3 wt.% at excess O_2 1 mol%) in the native state exhibit quite different patterns as shown in Figs. 2A and 3A, respectively. In comparison, the phase extraction nickel speciation data in Table 1 reveal 2.7- and 2.5-fold difference in total and soluble nickel, respectively, between ash #1 and ash #2. On the other hand, the speciation table shows similarity between ash #1 and ash #3 (from oil with sulfur 1.8 wt.% at excess O_2 2 mol%), and between ash #2 and ash #4 (from oil with sulfur 0.3 wt.% at excess O_2 3 mol%). Likewise, similarity is reflected when comparing the CV plots in Fig. 2A (ash #1) with Fig. 4A (ash #3) and Fig. 3A (ash #2) with Fig. 5A (ash #4). The potential range in A and B of Figs. 2–5 was expanded (-1.0 to $+1.0$ V) to observe the native ash and the step 1 residues over a wider potential scan. In no case was the anodic peak of Ni_3S_2 apparent in these ash plots. It appears that the broad features arising from the complex mixture of electroactive components present in the ash have obscured such recognition. Hence, stepwise phase extraction was carried out on each ash sample in an attempt to obtain more resolved voltammograms.

Upon extraction of water-soluble compounds from ash with pH 5 acetate solution in Step 1, various cathodic and anodic peaks disappeared in Figs. 3B and 5B (solid vs. dotted trace). Either a surface phase change had occurred on the native ash or water-soluble electroactive materials but not the sulfidic nickel were removed. Also, the

non-electroactive $NiSO_4$ shown in Fig. 1A should be extracted. This could result in CV either relatively unchanged (Fig. 2B) or even with current increase due to lesser non-electroactive components (Fig. 4B). With respect to the latter, the residue plot of ash #3 in Fig. 4B shows the emergence of an anodic peak at about −0.1 V. Since the best chance to observe the Ni_3S_2 anodic peak should be in the Step 2 residue, where the NiO–iron oxide phase is removed by the citrate-dithionite solution. Thus, Figs. 2C–5C for the four residues of Step 2 should be revealing. However, in all cases, there was a drastic reduction of redox current apparently due to removal of electroactive materials. Ni_3S_2, if present, should not be among the components removed in Step 2. None of these plots show any hint of the subsulfide anodic peak. Indeed, they resemble those in Figs. 2D–5D for the residues of Step 4, where the hydrogen peroxide treatment has removed the sulfides. No evidence can be found for the presence of Ni_3S_2 in these ash samples by the CPEV analysis. This solid state speciation of the oil ashes correlates with the extraction data in Table 1, which shows a small presence of sulfidic nickel ($< 2\%$ of the total Ni).

To verify that CPEV can detect Ni_3S_2 in the ash sample, a mixture of the #1 ash (10 mg) and Ni_3S_2 (1 mg) was prepared in a micromill and subjected to sequential extractions to obtain the residues. Fig. 6 shows the CPEV plots of the extraction residues of this Ni_3S_2-spiked ash #1. In Fig. 6A for the Step 1 residue, an anodic peak at about −0.05 V is visible, which becomes increasingly more resolved in Fig. 6B (−0.08 V) and Fig. 6C (−0.12 V) for the Step 2 and Step 3 residues, respectively. The latter is after electromagnetic extraction of metallic nickel, and the plot in Fig. 6C is reminiscent of the authentic Ni_3S_2 plot in Fig. 1B. The shift in the anodic peak potential from −0.05 to −0.12 V could come from a change in the double layer capacitance. The distinctive features of Ni_3S_2 disappeared in Fig. 6D for the Step 4 peroxide treatment residue, as expected.

In conclusion, the combined extraction–CPEV analyses of the residual oil ashes have not revealed detectable amount of Ni_3S_2. The solid state analyses of the EERC ash samples by CPEV are consistent with quantitative extractions of the nickel phases, showing $NiSO_4$ to be the predominant nickel species with very low proportions of sulfidic nickel. A similar observation was made by XAFS spectroscopic analysis of the same set of samples [7].

Acknowledgements

This work is supported by a research contract from the Electric Power Research Institute. We thank Kevin Galbreath of the Energy and Environmental Research Center, University of North Dakota, for the four oil ash samples used in this study.

References

[1] Federal Register 63 (22) (1998) February 3.
[2] National Toxicology Program Technical Report Series. No. 451, 453, 454, U.S. Dept. of Health and Human Services, 1996.

[3] J.L. Wong, J. Qian, C.H. Chen, Anal. Chim. Acta 349 (1997) 121.
[4] U.S. Environmental Protection Agency, Nickel subsulfide, in: Integrated Risk Information System,1988, CASRN 12035-72-2, IRIS, March 1.
[5] J.L. Wong, A.H. Liu, M. Tian, W.R. Jin, Fresenius' J. Anal. Chem 363 (1999) 572.
[6] R.N. Adams, Anal. Chem. 30 (1958) 1576.
[7] K.C. Galbreath, Z.J. Zygarlicke, F.E. Huggins, G.P. Huffman, J.L. Wong, Energy and Fuels 12 (1998) 818.
[8] Electric Power Research Institute, in: Electric Utility Trace Substances Synthesis Report Vol. 11994, EPRI TR-104614-V1, November.